

# Hyperthermia with Magnetic Nanowires for Inactivating Living Cells

D. S. Choi<sup>1,\*</sup>, J. Park<sup>2</sup>, S. Kim<sup>2</sup>, D. H. Gracias<sup>2</sup>, M. K. Cho<sup>3</sup>, Y. K. Kim<sup>3,†</sup>, A. Fung<sup>4</sup>,  
S. E. Lee<sup>5</sup>, Y. Chen<sup>4</sup>, S. Khanal<sup>1</sup>, S. Baral<sup>1</sup>, and J.-H. Kim<sup>1</sup>

<sup>1</sup>Department of Materials Science and Engineering, University of Idaho, Moscow, ID 83844

<sup>2</sup>Department of Chemical and Biomolecular Engineering, Johns Hopkins University, Baltimore, MD 21218, USA

<sup>3</sup>Department of Materials Science and Engineering, Korea University, Seoul 136-713, Korea

<sup>4</sup>Department of Biomedical Engineering, University of California, Los Angeles, CA 90095, USA

<sup>5</sup>Department of Mechanical and Aerospace Engineering, University of California, Los Angeles, CA 90095, USA

We describe a method to induce hyperthermia in cells, *in-vitro*, by remotely heating Ni nanowires (NWs) with radio frequency (RF) electromagnetic fields. Ni NWs were internalized by human embryonic kidney cells (HEK-293). Only cells proximal to NWs or with internalized NWs changed shape on exposure to RF fields indicative of cell death. The cell death occurs as a result of hyperthermia, since the RF field remotely heats the NWs as a result of magnetic hysteresis. This is the first demonstration of hyperthermia induced by NWs; since the NWs have anisotropic and strong magnetic moments, our experiments suggest the possibility of performing hyperthermia at lower field strengths in order to minimize damage to untargeted cells in applications such as the treatment of cancer.

## Keywords:

## 1. INTRODUCTION

Nanoparticles have been used in a wide range of diagnostic and therapeutic applications.<sup>1</sup> The small size of these particles coupled with surface functionalization have facilitated the concept of targeted medicine. Magnetic nanoparticles are especially attractive since they interact with remote electromagnetic fields in frequency ranges that penetrate a wide range of materials including tissue allowing the particles to be manipulated, tracked, imaged and remotely heated.<sup>2</sup> Magnetic nanoparticles have been utilized in a wide range of applications including cell sorting, as MRI contrast agents, remote controlled drug delivery and hyperthermia. Most of the nanoparticles used in these studies however have been approximately spherical or arbitrarily shaped faceted particles.

In this article, we have explored the use of magnetic nanowires (NWs) in hypothermia applications. While internalization of NWs in cells and manipulation of cells with NWs have been studied extensively,<sup>3–5</sup> to the best of our knowledge this is the first demonstration of hypothermic applications of NWs. As opposed to arbitrarily shaped magnetic nanoparticles, NWs have several advantages including favorable anisotropic magnetic properties, large

permanent magnetic moments (that decrease the field strengths required for heating), and increased surface area to volume ratio for more efficient targeting. Moreover, it is also known that nickel NWs are easily internalized by cells (due to Ni<sup>2+</sup> ions, also present in metalloproteins) and have no cytotoxicity, which has been attributed to the formation of several layers of nickel oxide.<sup>6</sup>

## 2. EXPERIMENTAL DETAILS

### 2.1. Nanowire Fabrication

For this study, Ni NWs were fabricated by electrodeposition using anodized aluminum oxide (AAO) nanopore membranes with a nominal pore diameter of 200 nm as templates. Anodization of aluminum foil was carried out with 0.3 M oxalic acid as an anodizing solution at room temperature. Details of anodization conditions for forming a variety of pore size are reported in our previous work.<sup>7</sup> Ni NWs were electrodeposited from a chloroplatinic acid bath with Boric acid (1 gL<sup>-1</sup> NiCl<sub>2</sub> hydrate and 25 gL<sup>-1</sup> Ni(H<sub>2</sub>NSO<sub>3</sub>)<sub>2</sub>, and H<sub>3</sub>BO<sub>3</sub> at pH 3.5 using an anodized aluminum foil having pores with a diameter of 200 nm. Prior to electrodeposition of Ni, a layer of gold was evaporated (200 nm thick) on one side of the alumina template and served as the conductive seed layer. The gold

\*Author to whom correspondence should be addressed.

†Co-corresponding author.

side of the alumina template was then adhered using carbon paste onto a supporting glass slide. Ni NWs were galvanostatically electrodeposited at a current density 35 mA/cm<sup>2</sup> at room temperature using a VMP2 Potentio/Galvanostat (Princeton Applied Research, Inc.). A piece of Pt coated Nb was used as a counter electrode. The length of the NWs was controlled by adjusting deposition time. After nanowire deposition, the anodized alumina template was removed with NaOH (20 wt%) to produce freestanding Ni NWs. Ni NWs were sterilized in Isopropanol Alcohol and transferred to culture media Dulbecco's modified Eagle's medium with 10% fetal bovine serum.

The structural information was obtained by X-ray diffractometry (XRD) and the magnetic properties were analyzed by a vibrating sample magnetometer (VSM). The microstructure of the NWs was analyzed by XRD (Cu K $\alpha$ ), field emission scanning electron microscopy (FESEM), and transmission electron microscopy (TEM). The magnetic properties of Ni nanowire arrays were characterized by a VSM with an external magnetic field of 1 kOe applied parallel and perpendicular to the nanowire axis, respectively.

### 3. RESULTS AND DISCUSSION

#### 3.1. Nanowire Characterization

Figure 1 shows the hysteresis loops for Ni nanowire arrays of (a) 90, and (b) 200 nm in diameter, respectively. Magnetic anisotropy developed as the nanowire diameter decreased, predominantly due to the shape effect. The coercivity ( $H_c$ ) and squareness ( $M_r/M_s$ ), i.e., the ratio between remanence and saturation magnetization, decreased as the nanowire diameter increased. Under the parallel field, the  $H_c$  and  $M_r/M_s$  values are 88 Oe and 0.09 for (a), and 86 Oe and 0.08 for (b), respectively.<sup>8</sup> Meanwhile, under the perpendicular field, the  $H_c$  and  $M_r/M_s$  values are 590 Oe and 0.33 for (a), and 540 Oe and 0.26 for (b), respectively.<sup>9</sup> Figure 2 shows the corresponding X-ray diffraction patterns of the Ni NWs. The  $\theta$ - $2\theta$  scan was performed with the scattering vector parallel to the plane of the AAO membrane. Both sample (a) and (b) show polycrystalline face-centered-cubic (fcc) phase. Figure 3 shows the high-resolution TEM image of a single Ni NW with diameter of 90 nm. The image suggests that the structure of the nanowire is polycrystalline with an fcc packing as confirmed by selected area electron diffraction (not shown here).

#### 3.2. Protein Adsorption onto Ni Nanowires

Ni NWs in IPA were precipitated by centrifugation at 1000 rpm for 5 min and resuspended in culture medium containing 10  $\mu$ g/ml Alexafluor 555-streptavidin conjugate (Invitrogen). The mixture was incubated at room temperature for 1 hour with agitation. The NWs were then

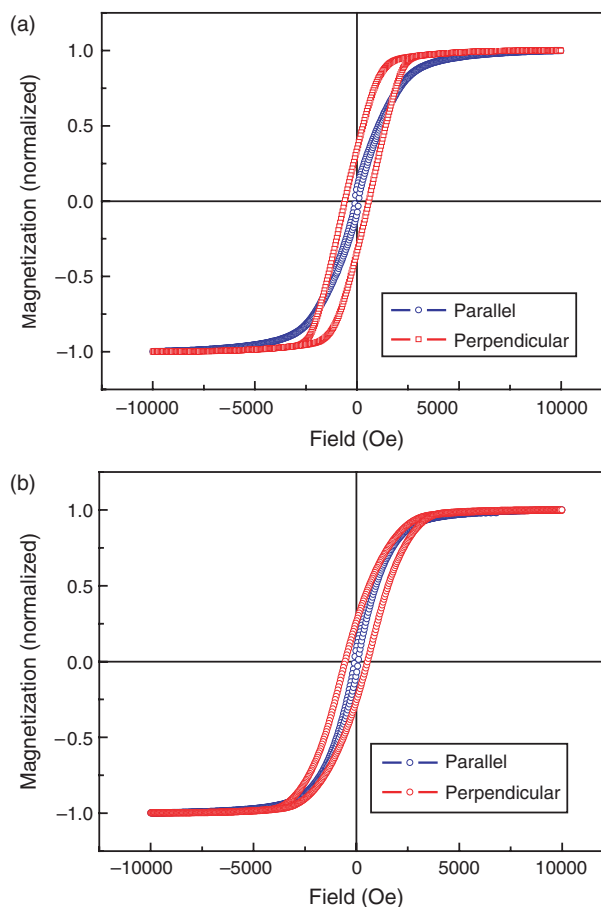


**Fig. 1.** Magnetic hysteresis loops for Ni nanowire arrays with diameters of (a) 90 nm, and (b) 200 nm under magnetic fields applied parallel and perpendicular to the nanowire axis.

centrifuged and resuspended in fresh DMEM twice more as described above to remove the trace IPA and unbound Alexafluor 555-streptavidin.

#### 3.3. Cell Culture and Incubation with Nanowires

Cell lines derived from human embryonic kidney (HEK-293) were purchased from American Type Culture Collection (ATCC). HEK-293 cells were grown in minimum essential medium (MEM) supplemented with 100 units/ml penicillin G, 100  $\mu$ g/ml streptomycin, 4 mM L-glutamine, and 10% fetal bovine serum (FBS). Cell cultures were split every 3–4 days, when they reached 70–80% confluency. At first, the medium was removed and the cells were washed once with prewarmed sterile PBS (containing no Ca<sup>2+</sup> and Mg<sup>2+</sup>). Secondly, 1–2 ml of trypsin-EDTA solution was added and treated for 1–2 min, or longer, until cells detached. To stop trypsinization, 5–10 ml of growth medium was added, and then the cells were resuspended gently but thoroughly. The desired number of viable cells was transferred to a new culture plate containing an appropriate volume of growth medium after counting cells. The plate was gently swirled to evenly distribute the cells. The

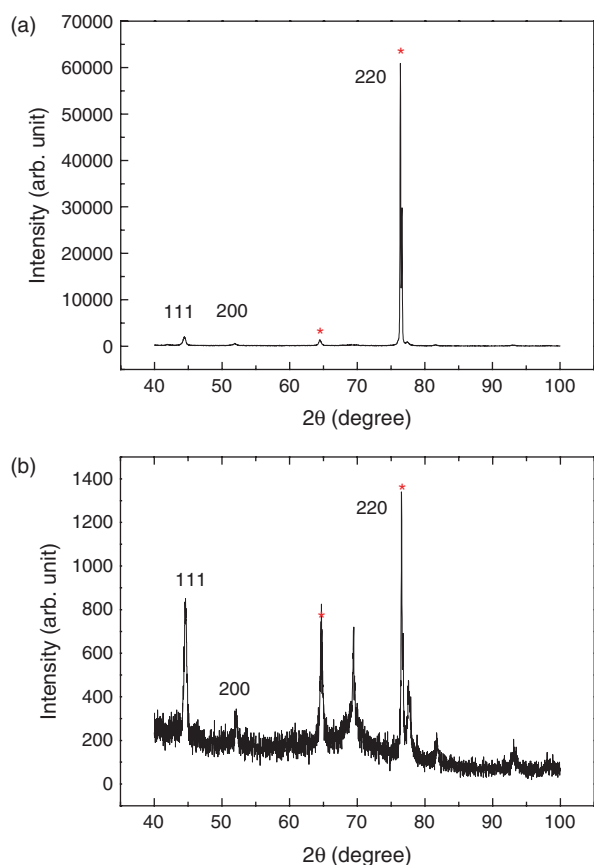


**Fig. 2.**  $\theta$ - $2\theta$  XRD spectra for Ni nanowire arrays with diameters of (a) 90 nm, and (b) 200 nm. Stars indicate Ag peaks from the electrode. The peak at  $70^\circ$  appearing in (b) is unidentified.

culture plate was placed in a  $37^\circ\text{C}$ , 5%  $\text{CO}_2$  humidified incubator. Following about 13 h incubation of cells with NWs, the cells were observed to have internalized many of the single and bundles of NWs as shown in Figure 4.

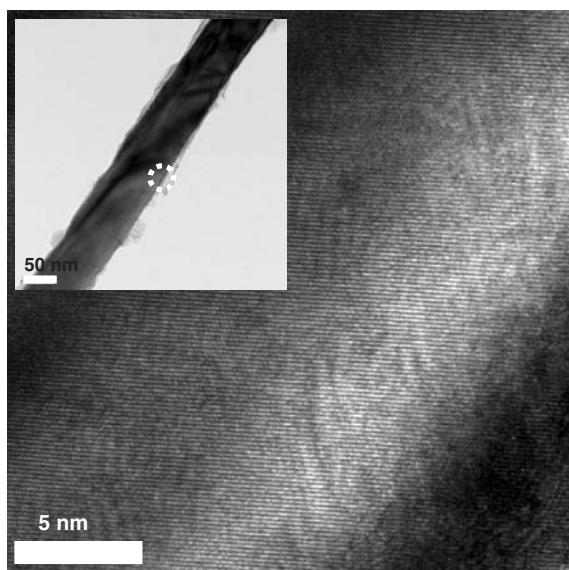


**Fig. 3.** TEM image at the edge of a single Ni nanowire with a diameter of 90 nm. Inset displays an image of the entire nanowire.

### 3.4. RF Heating Process for Inactivating the Living Cells

Hypothermia was induced in the cells using a remote radio frequency field. The schematic of the circuit diagram used to generate the RF field is shown in Figure 5. RF inductive heating occurred as a result of the electromagnetic

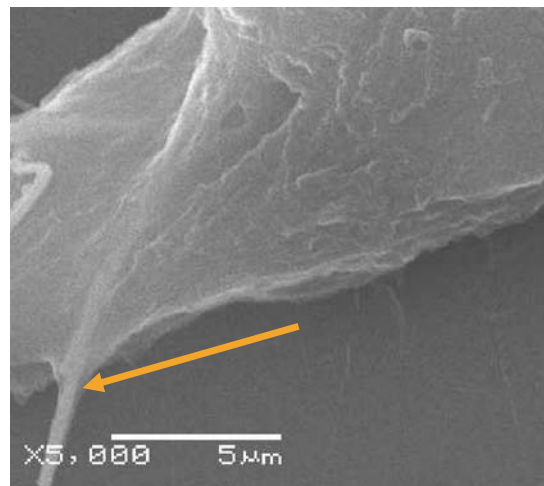


**Fig. 4.** FESEM micrograph of the cell bounded by Ni nanowires. The Ni nanowire is internalized by a cell as indicated by an arrow.

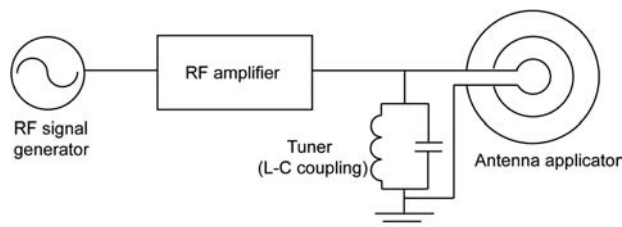


**Fig. 5.** Schematic of the circuit diagram used to generate the RF field required for hyperthermia.

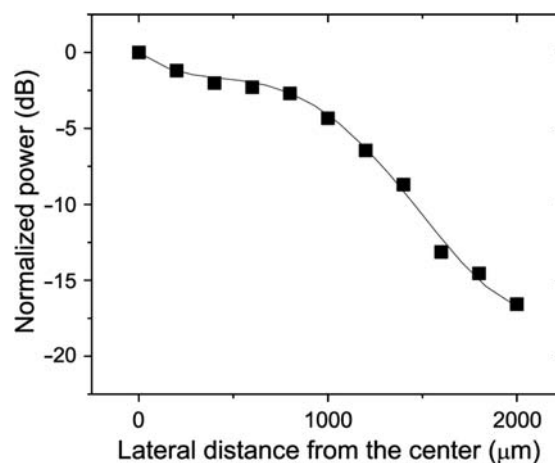


**Fig. 6.** The RF power coupling to the nanowires was simulated by HFSS. The output power is plotted along the lateral direction from the center of spiral antenna applicator. The normalized output power was slightly decreased up to the edge of outer ring and then falls off sharply.

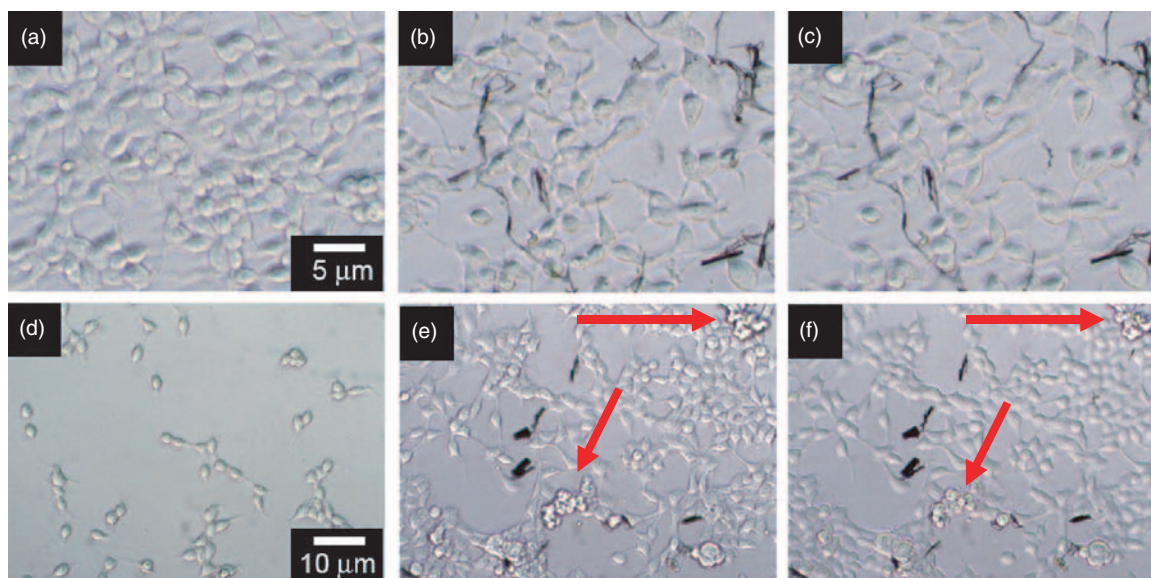


**Fig. 7.** The cell shape changed with RF inductive heating. (a) HEK-293 human kidney cells after 4 days of culture, (b) after 13 h incubation with nanowires, (c) nanowires kept for 4 min (d) HEK cells before the RF inductive heating process (e) nanowires attached to the cells and heated by RF inductive coupling for 2 min (f) nanowires heated by RF inductive coupling for 4 min. Arrows indicate the dead cells floating around in (e) and (f).

coupling between the NWs and the RF signal. The coupled electromagnetic field generated eddy currents on the surface of NWs which then heated up by the Joule effect. RF signal was generated by RF Signal Generator (RAMSEY RSG-1000B) at 810 MHz and tuned with Vector Network Analyzer (VNA). The RF signal can be amplified with RF power amplifier (American Microwave Technology 15100B) up to 10 W. The impedance of microstrip spiral antenna applicator was matched in L-C coupling circuit with double stub tuner (Weinschel, DS 109L) for the purposed frequency range. The desired impedance was determined by matching with  $50 \Omega$  load through the Smith Chart figure in VNA. As we have shown in the previous work<sup>10</sup> with remote heating of Ni microcontainers, the magnetic susceptibility of Ni is high, causing heating due to magnetic hysteresis. Figure 6 shows the simulation result of RF output power transferred into the NWs according to the off centered distance from the spiral applicator. The commercial electromagnetic simulator, high frequency structure simulator (HFSS, Ansoft Co.) was used for RF electromagnetic field analysis. The size of outmost ring of applicator set to  $1000 \mu\text{m}$ . The coupled electromagnetic field was analyzed with the finite element method while scanning longitudinally from the center point of spiral coil. The normalized output power was slightly decreased up to the edge of coil, (approx  $-5 \text{ dB}$ ) and then decreases sharply. The electromagnetic fields surrounding the coil were inversely proportioned to cubic distance from the coil so that the output power dropped to  $-18 \text{ dB}$  at a distance of  $2000 \mu\text{m}$ . From these simulations, we can correlate the coupling of RF radiation to the NWs to obtain the optimum RF coupling distance from the center of spiral antenna applicator.

The human kidney cells were inductively heated by RF power and *in-situ* image profiles of cell death process were imaged by a CCD camera. The structures of cells changed after heating as shown in Figure 7. Specifically, the human kidney cells were cultured in the petri dish and NWs were dispersed on the cells by micro-injection. After 2 minutes of heating, the shape of cells proximal to NWs deformed and floated around in dish as shown in Figure 7(e). The effects of RF heating on the cells were verified by comparing the cells without RF heating. The applied RF power was 3.5 W and transferred into the Ni NWs by the 2D RF coil.

#### 4. CONCLUSIONS

The results suggest that Ni NWs can be used for killing harmful cells with the selective functionalization followed by hyperthermia. We have demonstrated that human kidney cells were destroyed by the remotely coupled RF fields. We believe that the advantage of utilizing nanowires instead of nanoparticles is due to their high anisotropic magnetic moments possibly facilitating heating at lower fields, thereby minimizing damage to surrounding tissue. Since nanowires can also be fabricated in a multisegmented manner it is also possible to add additional functionality to the nanowires for sensing and optical imaging to construct multifunctional hyperthermia agents. As with other nanostructures chemical functionalization remains a challenging issue to target specific cells. Experiments for selectively killing cancer cells are in progress.

**Acknowledgments:** The authors gratefully acknowledge support for this work by the Director's Research and Development Fund 2006 and UI New Faculty

Start-up Fund. Y. K. Kim acknowledges the support of the Korea Science and Engineering Foundation grants M10633000049-06O3300-04910 (Pioneer Program), M10500000105-05J0000-10510 (National Research Laboratory Program), the Korea Research Foundation grant KRF-2004-005-D00057, and the Korea Health 21 R&D Project grant A050750. D. H. Gracias and J. Park acknowledge support from the NSF and the Beckman Foundation.

## References and Notes

1. F. Mauro, *Nat. Rev. Cancer* 5, 161 (2005).
2. Q. A. Pankhurst, J. Connolly, S. K. Jones, and J. Dobson, *J. Phys. D: Appl. Phys.* 36, R167 (2003).
3. N. J. Sniadecki, A. Anguelouch, M. T. Yang, C. M. Lamb, Z. Liu, S. B. Kirschner, Y. Liu, D. H. Reich, and C. S. Chen, *Proc. Natl. Acad. Sci. USA* 104, 14553 (2007).
4. M. Tanase, E. J. Felton, D. S. Gray, A. Hultgren, C. S. Chen, and D. H. Reich, *Lab Chip* 5, 598 (2005).
5. A. Hultgren, M. Tanase, C. S. Chen, G. J. Meyer, and D. H. Reich, *J. Appl. Phys.* 93, 7554 (2003).
6. P. Adriele, D. Zhu, C. John, and M. David, *J. Nanobiotechnol.* 4, 9 (2006).
7. N. Myung, J. Lim, J. Fleurial, M. Yun, and D. Choi, *Nanotechnology* 15, 1 (2004).
8. Y. K. Kim, J. Y. Soh, and D. Choi, Unpublished work (2006).
9. J. U. Cho, J. H. Min, S. P. Ko, J. Y. Soh, Y. K. Kim, J.-H. Wu, and S. H. Choi, *J. Appl. Phys.* 99, 08C909 (2006).
10. J. Park, D. A. Slanac, T. G. Leong, H. Ye, D. B. Nelson, and D. H. Gracias, *J. Microelectromech. Syst.* (2007), in press.

Received: 10 November 2007. Accepted: 7 January 2008.